

# Dispersion in Femtosecond Entangled Two-Photon Interference

Jan Peřina, Jr.\*<sup>†</sup>, Alexander V. Sergienko,  
Bradley M. Jost, Bahaa E. A. Saleh, Malvin C. Teich<sup>‡</sup>  
Quantum Imaging Laboratory<sup>§</sup>  
Department of Electrical and Computer Engineering  
Boston University  
8 Saint Mary's Street, Boston, MA 02215, USA

(short title: Entangled Two-Photon Interference)

Keywords: down-conversion, entangled two-photon interference, spontaneous processes, ultrafast nonlinear optics.

We theoretically investigate the quantum interference of entangled two-photon states generated in a nonlinear crystal pumped by femtosecond optical pulses. Interference patterns generated by the polarization analog of the Hong-Ou-Mandel interferometer are studied. Attention is devoted to the effects of the pump-pulse profile (pulse duration and chirp) and the second-order dispersion in both the nonlinear crystal and the interferometer's optical elements. Dispersion causes the interference pattern to have an asymmetric shape. Dispersion cancellation occurs in some cases.

## I. INTRODUCTION

Significant consideration has recently been given to the process of spontaneous parametric down-conversion in nonlinear crystals pumped by cw lasers [1,2,3,4]. The nonclassical properties of entangled two-photon light generated by this process have been used in many experimental schemes to elucidate distinctions between the predictions of classical and quantum physics [5]. Coincidence-count measurements with entangled two-photon states have revealed violations of Bell's inequalities [6], and have been considered for use in nonclassical imaging [7] and quantum cryptography [8].

A new frontier in these efforts is the generation of quantum states with three correlated particles (GHZ states) [9,10], which would be most useful for further tests of the predictions of quantum mechanics. One way to create such states is to make use of pairs of two-photon entangled states that are synchronized in time, i.e., generated within a sharp time window [11]. This can be achieved by using femtosecond pump beams. Also, successful quantum teleportation has already been observed using femtosecond pumping [12].

For these reasons, the theoretical and experimental properties of pulsed spontaneous parametric down-conversion have been scrutinized [13,14,15,16]. It has been shown that ultrashort pumping leads to a loss of visibility of the coincidence-count interference pattern in type-II parametric down-conversion [13,14,15], and narrowband frequency filters are required to restore the visibility [11,13,15].

This paper is devoted to a theoretical investigation of dispersion effects in femtosecond-pulsed spontaneous parametric down-conversion. Particular attention is given to the effects of pump-pulse chirp and second-order dispersion (in both the pump and down-converted beams) on the visibility and shape of the photon-coincidence pattern generated by the polarization analog of the Hong-Ou-Mandel interferometer [17]. Dispersion cancellation, which has been extensively studied in the case of cw pumping [18], is also predicted to occur under certain conditions for femtosecond down-converted pairs.

## II. SPONTANEOUS PARAMETRIC DOWN-CONVERSION WITH AN ULTRASHORT PUMP PULSE

We consider a nonlinear crystal pumped by a strong coherent-state field. Nonlinear interaction then leads to the spontaneous generation of two down-converted fields (the signal and the idler) which are mutually strongly correlated [1]. Such a correlation can be conveniently described in terms of the two-photon amplitude  $\mathcal{A}_{12}$  which is defined

---

\*On leave from the Joint Laboratory of Optics of Palacký University and Institute of Physics of Academy of Sciences of the Czech Republic, 17. listopadu 50, 772 07 Olomouc, Czech Republic.

<sup>†</sup>email: perina\_j@sloup.upol.cz

<sup>‡</sup>email: teich@bu.edu

<sup>§</sup>URL: <http://photon.bu.edu/teich/qil/QImaging.html>

as a matrix element of the product of electric-field operators  $\hat{E}_1^{(+)}(z_1, t_1)$  and  $\hat{E}_2^{(+)}(z_2, t_2)$  sandwiched between the entangled two-photon state  $|\psi^{(2)}\rangle$  (for details, see Appendix A) and the vacuum state  $|\text{vac}\rangle$ :

$$\mathcal{A}_{12}(z_1, t_1, z_2, t_2) = \langle \text{vac} | \hat{E}_1^{(+)}(z_1, t_1) \hat{E}_2^{(+)}(z_2, t_2) | \psi^{(2)}(0, t) \rangle. \quad (1)$$

The positive-frequency part  $\hat{E}_j^{(+)}$  of the electric-field operator of the  $j$ th beam is defined as

$$\hat{E}_j^{(+)}(z_j, t_j) = \sum_{k_j} e_j(k_j) f_j(\omega_{k_j}) \hat{a}_j(k_j) \exp(ik_j^v z_j - i\omega_{k_j} t_j), \quad j = 1, 2, \quad (2)$$

where  $\hat{a}_{k_j}$  stands for the annihilation operator of the mode with wave vector  $k_j$ ,  $e_j(k_j)$  denotes the normalization amplitude of the mode  $k_j$ , and  $f_j(\omega_{k_j})$  characterizes an external frequency filter placed in the  $j$ th beam. The symbols  $k_1^v$  and  $k_2^v$  denote wave vectors in vacuum.

At the termination of the nonlinear interaction in the crystal, the down-converted fields evolve according to free-field evolution and thus the two-photon amplitude  $\mathcal{A}_{12}$  depends only on the differences  $t_1 - t$  and  $t_2 - t$ . When the down-converted beams propagate through a dispersive material of the length  $l$ , the entangled two-photon state  $|\psi^{(2)}\rangle$  given in Eq. (A4) in Appendix A provides the expression for  $\mathcal{A}_{12,l}$ :

$$\begin{aligned} \mathcal{A}_{12,l}(\tau_1, \tau_2) = & C \int_{-L}^0 dz \sum_{k_p} \sum_{k_1} f_1(\omega_{k_1}) \sum_{k_2} f_2(\omega_{k_2}) \mathcal{E}_p^{(+)}(0, \omega_{k_p} - \omega_p^0) \exp[i(k_p - k_1 - k_2)z] \\ & \times \exp\left[i(\tilde{k}_1 + \tilde{k}_2)l\right] \delta(\omega_{k_p} - \omega_{k_1} - \omega_{k_2}) \exp[-i\omega_{k_1}\tau_1] \exp[-i\omega_{k_2}\tau_2]. \end{aligned} \quad (3)$$

The times  $\tau_1$  and  $\tau_2$  are given as follows:

$$-i\omega_{k_j}\tau_j = ik_j^v z_j - i\omega_{k_j}(t_j - t), \quad j = 1, 2. \quad (4)$$

The symbol  $\mathcal{E}_p^{(+)}(0, \omega_{k_p} - \omega_p^0)$  denotes the positive-frequency part of the envelope of the pump-beam electric-field amplitude at the output plane of the crystal and  $\omega_p^0$  stands for the central frequency of the pump beam; the wave vectors  $k_p$ ,  $k_1$ , and  $k_2$  ( $\tilde{k}_1$  and  $\tilde{k}_2$ ) are appropriate for the nonlinear crystal (dispersive material). The symbol  $L$  means the length of the crystal. The amplitudes  $e_1(k_1)$  and  $e_2(k_2)$  from Eq. (2) are absorbed into the constant  $C$ .

A typical experimental setup for coincidence-count measurement is shown in Fig. 1.

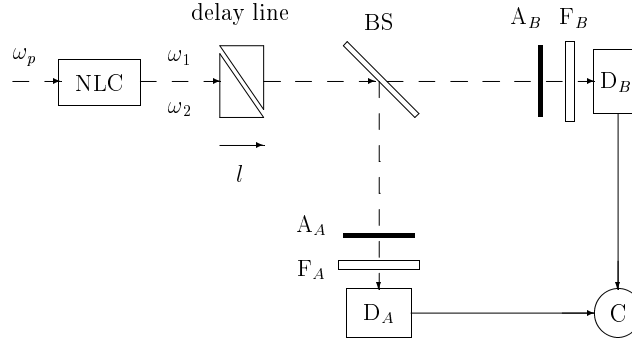


FIG. 1. Sketch of the system under consideration: a pump pulse at the frequency  $\omega_p$  generates down-converted photons at frequencies  $\omega_1$  and  $\omega_2$  in the nonlinear crystal NLC. These waves propagate through a delay line of length  $l$  and are detected at the detectors  $D_A$  and  $D_B$ ; BS denotes a beamsplitter;  $A_A$  and  $A_B$  are analyzers;  $F_A$  and  $F_B$  are frequency filters; and C indicates a coincidence device.

We consider type-II parametric down-conversion for this exposition. In this case two mutually perpendicularly polarized photons are provided at the output plane of the crystal. They propagate through a birefringent material of a variable length  $l$  and then impinge on a 50/50 beamsplitter. Finally they are detected at the detectors  $D_A$  and  $D_B$ . The coincidence-count rate  $R_c$  is measured by a coincidence device C. The beams might be filtered by the frequency filters  $F_A$  and  $F_B$  which can be placed in front of the detectors. Analyzers rotated by 45 degrees with respect to the ordinary and extraordinary axes of the nonlinear crystal enable quantum interference between two paths to be observed; either a photon from beam 1 is detected by the detector  $D_A$  and a photon from beam 2 by the detector  $D_B$ , or vice versa.

Including the effects of the beamsplitter and analyzers, the coincidence-count rate  $R_c$  can be determined as follows [13,14]:

$$R_c(l) = \frac{1}{4} \int_{-\infty}^{\infty} dt_A \int_{-\infty}^{\infty} dt_B |\mathcal{A}_{12,l}(t_A, t_B) - \mathcal{A}_{12,l}(t_B, t_A)|^2, \quad (5)$$

where the two-photon amplitude  $\mathcal{A}_{12,l}$  is given in Eq. (3).

The normalized coincidence-count rate  $R_n$  is then expressed in the form:

$$R_n(l) = 1 - \rho(l), \quad (6)$$

where

$$\rho(l) = \frac{1}{2R_0} \int_{-\infty}^{\infty} dt_A \int_{-\infty}^{\infty} dt_B \text{Re} [\mathcal{A}_{12,l}(t_A, t_B) \mathcal{A}_{12,l}^*(t_B, t_A)], \quad (7)$$

and

$$R_0 = \frac{1}{2} \int_{-\infty}^{\infty} dt_A \int_{-\infty}^{\infty} dt_B |\mathcal{A}_{12,l}(t_A, t_B)|^2. \quad (8)$$

The symbol Re denotes the real part of its argument.

### III. SPECIFIC MODELS INCLUDING SECOND-ORDER DISPERSION

Let us assume that the nonlinear crystal and the optical material in the path of the down-converted photons are both dispersive. We proceed to generalize the models provided in Refs. [13,14,15] by including the effects of second-order dispersion.

The wave vectors  $k_p(\omega_{k_p})$ ,  $k_1(\omega_{k_1})$ , and  $k_2(\omega_{k_2})$  of the beams in the nonlinear crystal can be expressed in the following form, when the effects of material dispersion up to the second order are included [19]:

$$k_j(\omega_{k_j}) = k_j^0 + \frac{1}{v_j}(\omega_{k_j} - \omega_j^0) + \frac{D_j}{4\pi}(\omega_{k_j} - \omega_j^0)^2, \quad j = p, 1, 2. \quad (9)$$

The inverse of group velocity  $1/v_j$ , and the second-order dispersion coefficient  $D_j$ , are given by

$$\frac{1}{v_j} = \left. \frac{dk_j}{d\omega_{k_j}} \right|_{\omega_{k_j}=\omega_j^0}, \quad (10)$$

$$D_j = 2\pi \left. \frac{d^2 k_j}{d\omega_{k_j}^2} \right|_{\omega_{k_j}=\omega_j^0}, \quad j = p, 1, 2. \quad (11)$$

The symbol  $\omega_j^0$  denotes the central frequency of beam  $j$ . The wave vector  $k_j^0$  is defined by the relation  $k_j^0 = k_j(\omega_j^0)$ .

Similarly, the wave vectors  $\tilde{k}_1(\omega_{k_1})$  and  $\tilde{k}_2(\omega_{k_2})$  of the down-converted beams in a dispersive material outside the crystal can be expressed as:

$$\tilde{k}_j(\omega_{k_j}) = \tilde{k}_j^0 + \frac{1}{g_j}(\omega_{k_j} - \omega_j^0) + \frac{d_j}{4\pi}(\omega_{k_j} - \omega_j^0)^2, \quad j = 1, 2, \quad (12)$$

where

$$\frac{1}{g_j} = \left. \frac{d\tilde{k}_j}{d\omega_{k_j}} \right|_{\omega_{k_j}=\omega_j^0}, \quad (13)$$

$$d_j = 2\pi \left. \frac{d^2 \tilde{k}_j}{d\omega_{k_j}^2} \right|_{\omega_{k_j}=\omega_j^0}, \quad j = 1, 2, \quad (14)$$

and  $\tilde{k}_j^0 = \tilde{k}_j(\omega_j^0)$ .

We further assume that frequency filters with a Gaussian profile, and centered around the central frequencies  $\omega_1^0$  and  $\omega_2^0$ , are incorporated:

$$f_j(\omega_{k_j}) = \exp \left[ -\frac{(\omega_{k_j} - \omega_j^0)^2}{\sigma_j^2} \right], \quad j = 1, 2, \quad (15)$$

where  $\sigma_j$  is the frequency width of the  $j$ th filter.

Assuming frequency- and wave-vector phase matching for the central frequencies ( $\omega_p^0 = \omega_1^0 + \omega_2^0$ ) and central wave vectors ( $k_p^0 = k_1^0 + k_2^0$ ), respectively, the two-photon amplitude  $\mathcal{A}_{12,l}(\tau_1, \tau_2)$  defined in Eq. (3) can be expressed in the form:

$$\begin{aligned} \mathcal{A}_{12,l}(\tau_1, \tau_2) &= C_A \exp(-i\omega_1^0\tau_1) \exp(-i\omega_2^0\tau_2) \int_{-L}^0 dz \int d\Omega_p \mathcal{E}_p^{(+)}(0, \Omega_p) \\ &\times \int d\Omega_1 \exp \left[ -\left( \frac{1}{\sigma_1^2} - i\frac{d_1 l}{4\pi} \right) \Omega_1^2 \right] \int d\Omega_2 \exp \left[ -\left( \frac{1}{\sigma_2^2} - i\frac{d_2 l}{4\pi} \right) \Omega_2^2 \right] \delta(\Omega_p - \Omega_1 - \Omega_2) \\ &\times \exp \left[ i \left( \frac{\Omega_p}{v_p} - \frac{\Omega_1}{v_1} - \frac{\Omega_2}{v_2} \right) z \right] \exp \left[ i \left( \frac{D_p}{4\pi} \Omega_p^2 - \frac{D_1}{4\pi} \Omega_1^2 - \frac{D_2}{4\pi} \Omega_2^2 \right) z \right] \\ &\times \exp \left[ -i \left( \tau_1 - \frac{l}{g_1} \right) \Omega_1 \right] \exp \left[ -i \left( \tau_2 - \frac{l}{g_2} \right) \Omega_2 \right]. \end{aligned} \quad (16)$$

The frequencies  $\Omega_j$ ,  $\Omega_j = \omega_{k_j} - \omega_j^0$ , for  $j = 1, 2, p$  have been introduced in Eq. (16);  $C_A$  denotes a constant.

We proceed to devote further attention to special cases. We first consider an ultrashort pump pulse with a Gaussian profile: the envelope  $\mathcal{E}_p^{(+)}(0, t)$  of the pump pulse at the output plane of the crystal then assumes the form [20]:

$$\mathcal{E}_p^{(+)}(0, t) = \xi_{p0} \exp \left( -\frac{1 + ia}{\tau_D^2} t^2 \right), \quad (17)$$

where  $\xi_{p0}$  is the amplitude,  $\tau_D$  is the pulse duration, and the parameter  $a$  describes the chirp of the pulse.

The complex spectrum  $\mathcal{E}_p^{(+)}(z, \Omega_p)$  of the envelope  $\mathcal{E}_p^{(+)}(z, t)$  is defined by

$$\mathcal{E}_p^{(+)}(z, \Omega_p) = \frac{1}{2\pi} \int_{-\infty}^{\infty} dt \mathcal{E}_p^{(+)}(z, t) \exp(i\Omega_p t). \quad (18)$$

For a pulse of the form given in Eq. (17) we obtain:

$$\mathcal{E}_p^{(+)}(0, \Omega_p) = \xi_p \frac{\tau_D}{2\sqrt{\pi} \sqrt[4]{1+a^2}} \exp \left[ -\frac{\tau_D^2}{4(1+a^2)} (1-ia)\Omega_p^2 \right], \quad (19)$$

where  $\xi_p = \xi_{p0} \exp[-i \arctan(a)/2]$ .

Substituting Eq. (19) into Eq. (16) and using the identity

$$\begin{aligned} \int_{-\infty}^{\infty} d\Omega_1 \int_{-\infty}^{\infty} d\Omega_2 \exp \left[ -\alpha_1 \Omega_1^2 - \alpha_2 \Omega_2^2 - 2\alpha_{12} \Omega_1 \Omega_2 + ia_1 \Omega_1 - ia_2 \Omega_2 \right] = \\ \frac{\pi}{\sqrt{\alpha_1 \alpha_2 - \alpha_{12}^2}} \exp \left[ -\frac{a_1^2 \alpha_2 + a_2^2 \alpha_1 + 2\alpha_{12} a_1 a_2}{4(\alpha_1 \alpha_2 - \alpha_{12}^2)} \right], \end{aligned} \quad (20)$$

we arrive at the following expression for the two-photon amplitude  $\mathcal{A}_{12,l}(\tau_1, \tau_2)$ :

$$\mathcal{A}_{12,l}(\tau_1, \tau_2) = C_A \frac{\xi_p \tau_D}{2\sqrt{\pi} \sqrt[4]{1+a^2}} \exp(-i\omega_1^0\tau_1) \exp(-i\omega_2^0\tau_2) A_{12,l}(\tau_1, \tau_2), \quad (21)$$

$$A_{12,l}(\tau_1, \tau_2) = \int_{-L}^0 dz \frac{1}{\sqrt{\beta_1 \beta_2 - \gamma^2}} \exp \left[ -\frac{c_1^2 \beta_2 + c_2^2 \beta_1 + 2\gamma c_1 c_2}{4(\beta_1 \beta_2 - \gamma^2)} \right]. \quad (22)$$

The functions  $\beta_j(z)$ ,  $c_j(z)$ , and  $\gamma(z)$  are defined as follows:

$$\begin{aligned}
\beta_j(z) &= \frac{1}{\sigma_j^2} + b(1 - ia) - i\frac{d_j}{4\pi}l - i\frac{D_p - D_j}{4\pi}z, & j = 1, 2 \\
c_j(z) &= (-1)^{(j-1)} \left[ \left( \frac{1}{v_p} - \frac{1}{v_j} \right) z + \frac{l}{g_j} - \tau_j \right], & j = 1, 2 \\
\gamma(z) &= b(1 - ia) - i\frac{D_p}{4\pi}z.
\end{aligned} \tag{23}$$

The parameter  $b$  is a characteristic parameter of the pump pulse:

$$b = \frac{\tau_D^2}{4(1 + a^2)}. \tag{24}$$

The quantities  $\rho(l)$  and  $R_0$  are then determined in accordance with their definitions in Eqs. (7) and (8), respectively. The quantity  $\rho(l)$  as a function of the length  $l$  of the birefringent material then takes the form ( $\omega_1^0 = \omega_2^0$  is assumed):

$$\rho(l) = \frac{\pi^2 |C_A|^2 |\xi_p|^2 \tau_D^2}{2\sqrt{1 + a^2} R_0} \operatorname{Re} \left\{ \int_{-L}^0 dz_1 \int_{-L}^0 dz_2 \frac{1}{\sqrt{\beta_1 \bar{\beta}_2 - \bar{\gamma}^2}} \exp \left[ -\frac{\bar{c}_1^2 \bar{\beta}_2 + \bar{c}_2^2 \bar{\beta}_1 + 2\bar{\gamma} \bar{c}_1 \bar{c}_2}{4(\beta_1 \bar{\beta}_2 - \bar{\gamma}^2)} \right] \right\}. \tag{25}$$

The functions  $\bar{\beta}_j(z_1, z_2)$ ,  $\bar{c}_j(z_1, z_2)$ , and  $\bar{\gamma}(z_1, z_2)$  are expressed as follows:

$$\begin{aligned}
\bar{\beta}_j(z_1, z_2) &= \frac{1}{\sigma_1^2} + \frac{1}{\sigma_2^2} - i\frac{d_j - d_{3-j}}{4\pi}l + 2b - i\frac{D_p - D_j}{4\pi}z_1 + i\frac{D_p - D_{3-j}}{4\pi}z_2, & j = 1, 2 \\
\bar{c}_j(z_1, z_2) &= \left( \frac{1}{v_p} - \frac{1}{v_1} \right) z_j - \left( \frac{1}{v_p} - \frac{1}{v_2} \right) z_{3-j} + \left( \frac{1}{g_1} - \frac{1}{g_2} \right) l, & j = 1, 2 \\
\bar{\gamma}(z_1, z_2) &= 2b - i\frac{D_p}{4\pi}(z_1 - z_2).
\end{aligned} \tag{26}$$

Similarly, the normalization constant  $R_0$  is given by the expression:

$$R_0 = \frac{\pi^2 |C_A|^2 |\xi_p|^2 \tau_D^2}{2\sqrt{1 + a^2}} \int_{-L}^0 dz_1 \int_{-L}^0 dz_2 \frac{1}{\sqrt{\tilde{\beta}_1 \tilde{\beta}_2 - \tilde{\gamma}^2}} \exp \left[ -\frac{\tilde{c}_1^2 \tilde{\beta}_2 + \tilde{c}_2^2 \tilde{\beta}_1 + 2\tilde{\gamma} \tilde{c}_1 \tilde{c}_2}{4(\tilde{\beta}_1 \tilde{\beta}_2 - \tilde{\gamma}^2)} \right], \tag{27}$$

where

$$\begin{aligned}
\tilde{\beta}_j(z_1, z_2) &= \frac{2}{\sigma_j^2} + 2b - i\frac{D_p - D_j}{4\pi}(z_1 - z_2), & j = 1, 2 \\
\tilde{c}_j(z_1, z_2) &= \left( \frac{1}{v_p} - \frac{1}{v_j} \right) (z_j - z_{3-j}), & j = 1, 2 \\
\tilde{\gamma}(z_1, z_2) &= 2b - i\frac{D_p}{4\pi}(z_1 - z_2).
\end{aligned} \tag{28}$$

It is convenient to consider the pump pulse characteristics at the output plane of the crystal, i.e., to use the parameters  $\tau_D$  and  $a$ . They can be expressed in terms of the parameters  $\tau_{Di}$  and  $a_i$  appropriate for the input plane of the crystal:

$$\begin{aligned}
a &= \left( \frac{\tau_{Di}^2 a_i}{4(1 + a_i^2)} + \frac{D_p L}{4\pi} \right) \left( \frac{\tau_{Di}^2}{4(1 + a_i^2)} \right)^{-1}, \\
\tau_D &= \tau_{Di} \sqrt{\frac{1 + a^2}{1 + a_i^2}}.
\end{aligned} \tag{29}$$

In this case, the parameter  $b_i$

$$b_i = \frac{\tau_{Di}^2}{4(1 + a_i^2)} \tag{30}$$

has the same value as the parameter  $b$  defined in Eq. (24).

Ignoring second-order dispersion in all modes ( $D_p = D_1 = D_2 = 0$ ), Eq. (25) reduces to the following analytical expression for the quantity  $\rho$ :

$$\rho(\Delta\tau_l) = \sqrt{\frac{\pi}{2}} \frac{1}{|\Lambda|L} \frac{\tau_{Di}}{\sqrt{1+a_i^2}} \operatorname{erf} \left[ \frac{\sqrt{2}|\Lambda|}{D} \frac{\sqrt{1+a_i^2}}{\tau_{Di}} \left( \frac{DL}{2} - |\Delta\tau_l| \right) \right], \quad (31)$$

in which

$$\begin{aligned} D &= \frac{1}{v_1} - \frac{1}{v_2}, \\ \Lambda &= \frac{1}{v_p} - \frac{1}{2} \left( \frac{1}{v_1} + \frac{1}{v_2} \right), \end{aligned} \quad (32)$$

and

$$\Delta\tau_l = \tau_l - DL/2. \quad (33)$$

The symbol erf denotes the error function. When deriving Eq. (31) the condition  $D > 0$  was assumed. In Eq. (33),  $\tau_l$  denotes the relative time delay of the down-converted beams in a birefringent material of length  $l$  and is defined as follows:

$$\tau_l = \left( \frac{1}{g_2} - \frac{1}{g_1} \right) l. \quad (34)$$

When second-order dispersion in the down-converted fields is omitted, the interference pattern can be determined for an arbitrary pump-pulse profile in terms of the autocorrelation function of the pump pulse. For details, see Appendix B.

#### IV. DISCUSSION

We now proceed to examine the behavior of the normalized coincidence-count rate  $R_n$  on various parameters, from both analytical and numerical points of view.

The profile of the interference dip in the coincidence-count rate [17] (described by  $\rho$  as a function of  $l$ ), formed by the overlap of a pair of two-photon amplitudes, can be understood as follows. The expression in Eq. (7) for  $\rho(l)$  can be rewritten in the form:

$$\rho(l) = \frac{1}{2R_0} \int_{-\infty}^{\infty} dt \int_{-\infty}^{\infty} d\tau [\mathcal{A}_{12,l}^r(t,\tau)\mathcal{A}_{12,l}^r(t,-\tau) + \mathcal{A}_{12,l}^i(t,\tau)\mathcal{A}_{12,l}^i(t,-\tau)], \quad (35)$$

where

$$t = \frac{t_A + t_B}{2}, \quad \tau = t_A - t_B, \quad (36)$$

and  $\mathcal{A}_{12,l}^r = \operatorname{Re}[\mathcal{A}_{12,l}]$ ;  $\mathcal{A}_{12,l}^i = \operatorname{Im}[\mathcal{A}_{12,l}]$ . The symbol Im denotes the imaginary part of the argument. Hence, according to Eq. (35), the overlaps of the real and imaginary parts of the two-photon amplitudes  $\mathcal{A}_{12,l}(t,\tau)$  and  $\mathcal{A}_{12,l}(t,-\tau)$  determine the values of the interference term  $\rho$ . The amplitude  $\mathcal{A}_{12,l}(t,-\tau)$  can be considered as a mirror image of the amplitude  $\mathcal{A}_{12,l}(t,\tau)$  with respect to the plane  $\tau = 0$ . When only first-order dispersion in the optical material is taken into account, the shape of the two-photon amplitude  $\mathcal{A}_{12,l}(t,\tau)$  does not depend on the length  $l$ ; as  $l$  increases, the amplitude  $\mathcal{A}_{12,l}(t,\tau)$  moves only in the  $t$ - $\tau$  plane. The shift in the  $\tau$ -direction is important, because it changes the degree of overlap of the amplitudes. This reveals the origin of the shape of the dip.

The overlap of the two-photon amplitudes can be interpreted from the point-of-view of distinguishability of two paths leading to coincidence detection [13]. When the overlap is complete, the two paths cannot be distinguished and the interference pattern has maximum visibility. Incomplete overlap means that the paths can be ‘‘partially distinguished’’ and thus the visibility is reduced.

We consider, in turn, the role played by pump-pulse duration and chirp, second-order dispersion in the nonlinear down-converting medium, second-order dispersion in the optical elements of the interferometer, and dispersion cancellation.

### A. Pump-pulse duration and chirp

In the absence of second-order dispersion and frequency filters, a useful analytical expression for the two-photon amplitude  $A_{12,l=0}(t, \tau)$  can be obtained:

$$A_{12,l=0}(t, \tau) = \frac{4\pi\sqrt{\pi}^4\sqrt{1+a_i^2}}{\tau_{Di}|D|} \text{rect}\left(\frac{\tau}{DL}\right) \exp\left[-\frac{1+ia_i}{\tau_{Di}^2}\left(t + \frac{\Lambda}{D}\tau\right)^2\right]. \quad (37)$$

The coefficients  $D$  and  $\Lambda$  are defined in Eq. (32). Equation (37) elucidates the role of pump-pulse parameters as discussed below. It is well known that for a cw-pump field the coincidence-count rate  $R_n(\tau_l)$  forms a triangular dip of width  $DL$  [1]. The visibility is 100%, indicating maximum interference. An ultrashort pump pulse of duration  $\tau_{Di}$  leads to a loss of visibility (see Fig. 2) but the width of the dip remains unchanged [13]. This can be understood from the shape of the two-photon amplitude  $A_{12,l=0}(t, \tau)$  given in Eq. (37). In the  $\tau$ -direction the two-photon amplitude is confined to the region  $0 < \tau < DL$  for either cw or an ultrashort pump pulse; this confinement is responsible for the width of the dip. The two-photon amplitude is confined in the  $t$ -direction by the ultrashort pump-pulse duration [see Eq. (37)]. The tilt (given by the ratio  $\Lambda/D$ , see Eq. (37)) of the amplitude in the  $t$ - $\tau$  plane leads to a loss of visibility since the overlap of the amplitudes  $A_{12,l}(t, \tau)$  and  $A_{12,l}(t, -\tau)$  for a given optimum value of  $l$  cannot be complete for a nonzero tilt. The shorter the pump-pulse duration, the smaller the overlap, and the lower values of visibility that result. However, when values of the first-order dispersion parameters are chosen such that  $\Lambda = 0$ , the tilt is zero [see Eq. (37)] and no loss of visibility occurs as the pump-pulse duration shortens (for details, see [14]).

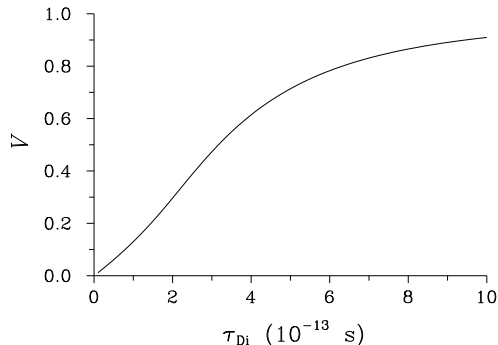


FIG. 2. Visibility  $\mathcal{V}$  ( $\mathcal{V} = \rho/(2 - \rho)$ ) as a function of the pump-pulse duration  $\tau_{Di}$ ;  $L = 3$  mm,  $\sigma = \infty$  nm, and  $a_i = 0$ ; values of the other parameters are zero. In Figs. 2–8, the following parameters apply. Values of the inverse group velocities appropriate for the BBO crystal with type-II interaction at the pump wavelength  $\lambda_p = 397.5$  nm, and at down-conversion wavelengths  $\lambda_1 = \lambda_2 = 795$  nm are:  $1/v_p = 57.05 \times 10^{-13}$  s/mm,  $1/v_1 = 56.2 \times 10^{-13}$  s/mm, and  $1/v_2 = 54.26 \times 10^{-13}$  s/mm. We assume that the optical materials for the interferometer are quartz, for which  $1/g_1 = 51.81 \times 10^{-13}$  s/mm and  $1/g_2 = 52.08 \times 10^{-13}$  s/mm.

As indicated by the Eq. (37) for the amplitude  $A_{12,l=0}$ , pump-pulse chirp (characterized by  $a_i$ ) introduces a phase modulation of the two-photon amplitude in the  $t$ -direction. This modulation decreases the overall overlap of the corresponding two-photon amplitudes, given as a sum of the overlaps of their real and imaginary parts. Increasing values of the chirp parameter  $a_i$  thus lead to a reduction of visibility. However, the width of the dip does not change. In fact, it is the parameter  $b_i$  given in Eq. (30), combining both the pulse duration  $\tau_{Di}$  and the chirp parameter  $a_i$ , that determines the visibility in case of a Gaussian pump pulse. To be more specific the parameter  $b_i$  is determined by the bandwidth  $\Delta\Omega_p$  [ $\Delta\Omega_p = \sqrt{2}\sqrt{1+a_i^2}/\tau_{Di}$ , see Eq. (19)] of the pump pulse according to the relation  $b_i = 1/[2(\Delta\Omega_p)^2]$ . Thus, more generally, it is the bandwidth of the pump pulse that determines the interference pattern. As a consequence, dispersion of the pump beam between the pump-pulse source and the nonlinear crystal does not influence the interference pattern.

Examination of Eqs. (B3) and (B4) in Appendix B shows that the dip remains symmetric since the function  $\rho(\Delta\tau_l)$  in Eq. (B3) is an odd function of  $\Delta\tau_l$  for an arbitrary pump-pulse profile.

Frequency filters inserted into the down-converted beams serve to broaden the two-photon amplitude  $A_{12,l}(t, \tau)$  both in the  $t$ - and  $\tau$ -direction. Broadening in the  $\tau$ -direction leads to wider dips, whereas that in the  $t$ -direction smooths out the effect of tilt discussed above and thereby results in a higher visibility. The narrower the spectrum of frequency filters, the wider the dip, and the higher the observed visibility. The effect of chirp is suppressed by the presence of frequency filters, because they effectively make the complex pump-pulse spectrum narrower and hence diminish relative phase changes across such a narrowed complex spectrum.

## B. Second-order dispersion in the nonlinear crystal

Second-order dispersion in the *pump beam* causes changes in the pulse phase (chirp) as the pulse propagates and this leads to broadening of the pulse. The effect of such pump-pulse broadening is transferred to the down-converted beams, as is clearly shown by the behavior of the two-photon amplitude  $A_{12,l}(t, \tau)$  illustrated in Fig. 3.

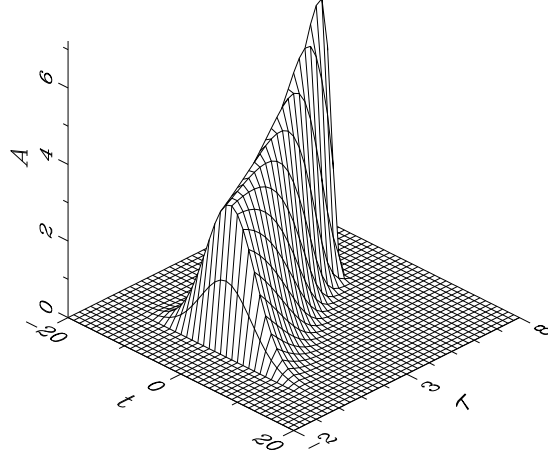


FIG. 3. Absolute value of the two-photon amplitude  $A = |A_{12,l=0}(t, \tau)|$  for nonzero second-order dispersion of the pump beam; the variables  $t$  and  $\tau$  are in units of  $10^{-13}$  s;  $\tau_{Di} = 1.55 \times 10^{-13}$  s,  $L = 3$  mm,  $\sigma = 100$  nm,  $D_p = 1 \times 10^{-25}$  s<sup>2</sup>/mm, and  $a_i = 0$ ; values of the other parameters are zero.

In this figure, the amplitude in the region near  $\tau = 0$  s has its origin near the output plane of the crystal where the pump pulse is already broadened as a result of its having propagated through the dispersive crystal. At the other edge, near  $\tau \approx 6 \times 10^{-13}$  s the down-converted light arises from the beginning of the crystal where the pump pulse has not yet suffered dispersive broadening. The profile of the interference dip is modified as follows: An increase in the second-order dispersion parameter  $D_p$  leads to an increase of visibility, but no change in the width of the dip, as illustrated in Fig. 4(a). For appropriately chosen values of  $D_p$  a small local peak emerges at the bottom of the dip [see Fig. 4(a)]. Nonzero initial chirp ( $a_i$ ) of the pump beam can provide a higher central peak but on the other hand it reduces the visibility [see Fig. 4(b)]. The peak remains, but is suppressed, in the presence of narrow frequency filters.

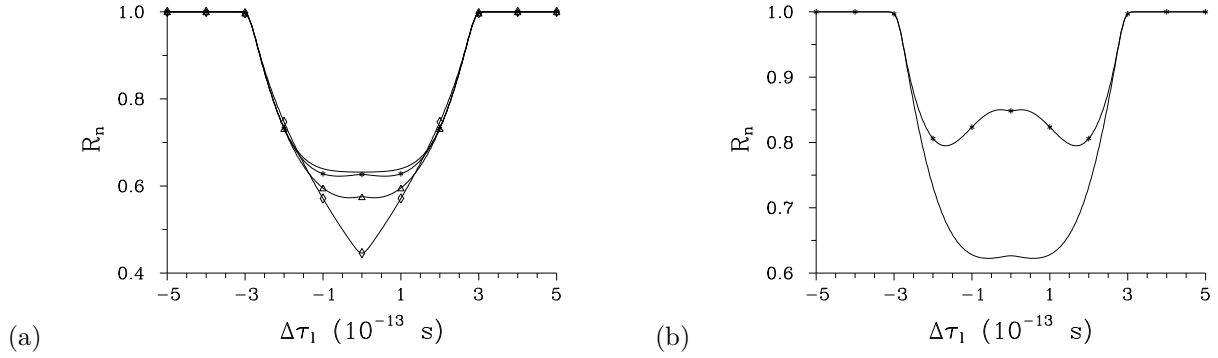


FIG. 4. Coincidence-count rate  $R_n(\Delta\tau_1)$  (a) for various values of the second-order dispersion parameter  $D_p$ :  $D_p = 0$  s<sup>2</sup>/mm (plain curve),  $D_p = 5 \times 10^{-26}$  s<sup>2</sup>/mm (\*),  $D_p = 1 \times 10^{-25}$  s<sup>2</sup>/mm ( $\Delta$ ), and  $D_p = 3 \times 10^{-25}$  s<sup>2</sup>/mm ( $\diamond$ ),  $a_i = 0$  and (b) for various values of the chirp parameter  $a_i$ :  $a_i = 0$  (plain curve) and  $a_i = 2$  (\*),  $D_p = 5 \times 10^{-26}$  s<sup>2</sup>/mm;  $\tau_{Di} = 1.55 \times 10^{-13}$  s;  $L = 3$  mm;  $\sigma = 50$  nm; values of the other parameters are zero.

Now we turn to second-order dispersion in the *down-converted beams* (nonzero  $D_1, D_2$ ), which broadens the two-photon amplitude  $A_{12,l}(t, \tau)$  in the  $\tau$ -, as well as in the  $t$ -direction. As demonstrated in Fig. 5, this leads to a broadening of the dip, as well as asymmetry and oscillations at its borders. When values of  $D_1$  increase, visibility decreases at first and then later increases. Nonzero chirp leads to a lower visibility, but tends to suppress oscillations at the borders of the dip. Frequency filters, which behave as discussed above, suppress asymmetry.



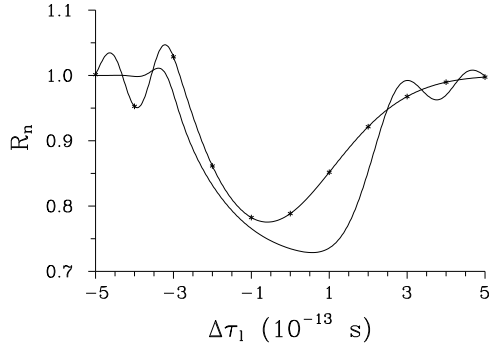


FIG. 5. Coincidence-count rate  $R_n(\Delta\tau_1)$  in case of second-order dispersion in beam 1 (plain curve,  $D_1 = 1 \times 10^{-25} \text{ s}^2/\text{mm}$ ,  $D_2 = 0 \text{ s}^2/\text{mm}$ ) and in beam 2 (\*,  $D_1 = 0 \text{ s}^2/\text{mm}$ ,  $D_2 = 1 \times 10^{-25} \text{ s}^2/\text{mm}$ );  $\tau_{Di} = 1.55 \times 10^{-13} \text{ s}$ ,  $L = 3 \text{ mm}$ , and  $\sigma_1 = \sigma_2 = 50 \text{ nm}$ ; values of the other parameters are zero.

When second-order dispersion occurs in all three modes, the two-photon amplitude  $A_{12,i}(t, \tau)$  is broadened for smaller values of  $\tau$  (mainly owing to dispersion in the pump beam) as well as for greater values of  $\tau$  (mainly owing to dispersion in the down-converted beams). As a result, the interference pattern comprises all of the features discussed above: a local peak may emerge at the bottom of the dip, the dip is broadened and asymmetric, and there occur oscillations at the borders of the dip.

To observe the above mentioned effects caused by dispersion in a nonlinear crystal, relatively large values of the dispersion parameters  $D_p$ ,  $D_1$ , and  $D_2$  are required. For example, our simulations make use of parameter values that are approximately an order of magnitude higher than those of the BBO crystals commonly used in type-II down-conversion-based interferometric experiments.

### C. Second-order dispersion in the interferometer's optical elements

Second-order dispersion in an optical material ( $d_1, d_2$ ) through which down-converted photons propagate leads to asymmetry of the dip. The dip is particularly stretched to larger values of  $l$  (see Fig. 6) as a consequence of the deformation and lengthening of the two-photon amplitude  $A_{12,i}$  in a dispersive material. The higher the difference  $d_1 - d_2$  of the dispersion parameters, the higher the asymmetry and the wider the dip; moreover its minimum is shifted further to smaller values of  $l$  (see Fig. 6). Asymmetry of the dip is also preserved when relatively narrow frequency filters are used though the narrowest filters remove it. Chirp decreases visibility but the shape of the dip remains unchanged.

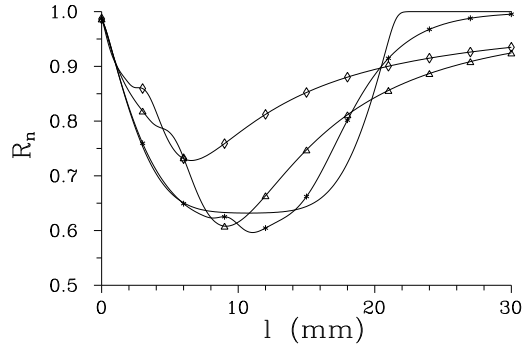


FIG. 6. Coincidence-count rate  $R_n(l)$  for various values of the second-order dispersion parameter  $d = d_1 - d_2$  of an optical material;  $d = 0 \text{ s}^2/\text{mm}$  (plain curve),  $d = 1 \times 10^{-26} \text{ s}^2/\text{mm}$  (\*),  $d = 5 \times 10^{-26} \text{ s}^2/\text{mm}$  ( $\Delta$ ), and  $d = 1 \times 10^{-25} \text{ s}^2/\text{mm}$  ( $\diamond$ );  $\tau_{Di} = 1.55 \times 10^{-13} \text{ s}$ ,  $L = 3 \text{ mm}$ , and  $\sigma_1 = \sigma_2 = 50 \text{ nm}$ ; values of the other parameters are zero.

### D. Dispersion cancellation

Asymmetry of the dip caused by second-order dispersion in an optical material through which down-converted photons propagate can be suppressed in two cases. In the first case, for a pump pulse of arbitrary duration, dispersion

cancellation occurs when the magnitude of second-order dispersion in the path of the first photon (given by  $d_1l$ ) equals that of the second photon (given by  $d_2l$ ). This observation immediately follows from Eqs. (25) and (26), in which the effect of second-order dispersion is prescribed by the parameter  $(d_1 - d_2)l$ . Dispersion cancellation is a result of completely destructive interference between the amplitudes  $A_{12,i}(t, \tau)$  and  $A_{12,i}(t, -\tau)$  for which there is nonzero overlap. This is demonstrated in Fig. 7 for  $l = 25$  mm, i.e. for which  $\rho = 0$ .

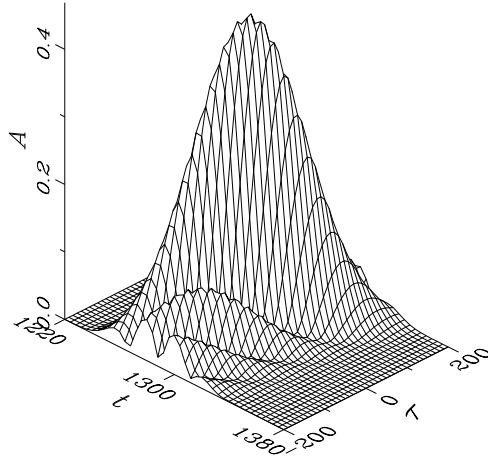


FIG. 7. Absolute value of the two-photon amplitude  $A = |A_{12,i}(t, \tau)|$  for the same amount of second-order dispersion in the down-converted beams ( $d_1 = d_2 = 1 \times 10^{-25}$  s<sup>2</sup>/mm) for  $l = 25$  mm; the variables  $t$  and  $\tau$  are in units of  $10^{-13}$  s;  $\tau_{Di} = 1.55 \times 10^{-13}$  s,  $L = 3$  mm, and  $\sigma = 100$  nm; values of the other parameters are zero.

When the pulse duration is sufficiently long (in the cw regime) dispersion cancellation occurs for arbitrary magnitudes of second-order dispersion (given by  $d_1l$  and  $d_2l$ ) present in the paths of the down-converted photons. The gradual suppression of the asymmetry of the dip as the pump pulse duration increases is shown in Fig. 8.

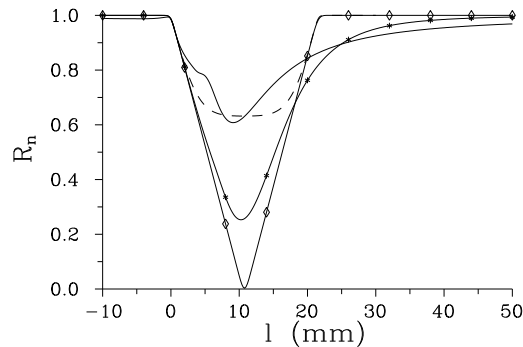


FIG. 8. Coincidence-count rate  $R_n(l)$  shows a gradual suppression of dispersion effects (asymmetry) as the pump-pulse duration increases;  $\tau_{Di} = 1.55 \times 10^{-13}$  s (plain solid curve),  $\tau_{Di} = 5 \times 10^{-13}$  s (\*), and  $\tau_{Di} = 1 \times 10^{-11}$  s ( $\diamond$ ),  $d = d_1 - d_2 = 5 \times 10^{-26}$  s<sup>2</sup>/mm; for comparison  $\tau_{Di} = 1.55 \times 10^{-13}$  s,  $d = 0$  s<sup>2</sup>/mm (dashed curve);  $L = 3$  mm;  $\sigma_1 = \sigma_2 = 50$  nm; values of the other parameters are zero.

Dispersion cancellation has its origin in the entanglement of the photons, i.e., in the fact that the permitted values of the frequency  $\omega_1$  and the frequency  $\omega_2$  are governed by the relation  $\delta(\omega_p - \omega_1 - \omega_2)$ , where  $\omega_p$  lies within the pump-pulse spectrum.

## V. CONCLUSION

We have developed a description of two-photon type-II spontaneous parametric down-conversion produced when ultrashort pulses from a femtosecond laser are used to pump an appropriate nonlinear medium, as well as the associated two-photon interference effects. The model includes frequency modulation of the pump pulse (chirp) and dispersion in both the nonlinear crystal and the interferometer's optical elements. The influence of these features on the depth

and asymmetry characteristics of a photon-coincidence interference dip have been established.

We showed that the interference pattern is determined by the bandwidth of the pump pulse; the larger the bandwidth, the lower the interference-pattern visibility. This implies that dispersion of the pump beam before the nonlinear crystal does not influence the interference pattern. Second-order dispersion of the pump beam in the nonlinear crystal can result in the occurrence of a local peak at the bottom of the interference dip. Second-order dispersion of the down-converted photons in the crystal can result in oscillations at the borders of the dip, whereas dispersion of the down-converted photons in the interferometer's optical materials (e.g., the delay line) can produce an asymmetry in the dip. These effects can be used to measure the dispersion parameters of both a nonlinear crystal and an arbitrary optical material. Dispersion cancellation has been revealed for pump pulses of arbitrary duration when the amount of dispersion in the two down-converted beams is identical and in general for sufficiently long pump pulses.

## ACKNOWLEDGMENTS

The authors thank J. Peřina and M. Atature for valuable discussions. This work was supported by the National Science Foundation under Grant Nos. ECS-9800300 and ECS 9810355. J. P. acknowledges support from Grant No. VS96028 of the Czech Ministry of Education.

## APPENDIX A: DETERMINATION OF AN ENTANGLED TWO-PHOTON STATE

The interaction Hamiltonian of the process of spontaneous parametric down-conversion can be written in the form [1]:

$$\hat{H}_{\text{int}}(t) = \int_{-L}^0 dz \chi^{(2)} E_p^{(+)}(z, t) \hat{E}_1^{(-)}(z, t) \hat{E}_2^{(-)}(z, t) + \text{h.c.}, \quad (\text{A1})$$

where  $\chi^{(2)}$  is the second-order susceptibility,  $E_p^{(+)}$  denotes the positive-frequency part of the electric-field amplitude of the pump field, and  $E_1^{(-)}$  ( $E_2^{(-)}$ ) is the negative-frequency part of the electric-field operator of down-converted field 1 (2). The nonlinear crystal extends from  $z = -L$  to  $z = 0$ . The symbol h.c. means Hermitian conjugate.

Expanding the interacting fields into harmonic plane waves, the interaction Hamiltonian  $\hat{H}_{\text{int}}$  in Eq. (A1) can be recast into the form:

$$\begin{aligned} \hat{H}_{\text{int}}(t) = C_{\text{int}} \int_{-L}^0 dz \sum_{k_p} \sum_{k_1} \sum_{k_2} \chi^{(2)} \mathcal{E}_p^{(+)}(0, \omega_{k_p} - \omega_p^0) \hat{a}_1^\dagger(k_1) \hat{a}_2^\dagger(k_2) \\ \times \exp [i(k_p - k_1 - k_2)z - i(\omega_{k_p} - \omega_{k_1} - \omega_{k_2})t] + \text{h.c.}, \end{aligned} \quad (\text{A2})$$

where  $C_{\text{int}}$  is a constant. The symbol  $\mathcal{E}_p^{(+)}(0, \omega_{k_p} - \omega_p^0)$  denotes the positive-frequency part of the envelope of the pump-beam electric-field amplitude at the output plane of the crystal;  $k_p$  stands for the wave vector of a mode in the pump beam, and  $\omega_p^0$  stands for the central frequency of the pump beam. The symbol  $\hat{a}_1^\dagger(k_1)$  ( $\hat{a}_2^\dagger(k_2)$ ) represents the creation operator of the mode with wave vector  $k_1$  ( $k_2$ ) and frequency  $\omega_{k_1}$  ( $\omega_{k_2}$ ) in the down-converted field 1 (2). We note that the phases of all three interacting fields in space are chosen in such a way that they are zero at the output plane of the crystal.

The wave function  $|\psi^{(2)}(0, t)\rangle$  describing an entangled two-photon state whose phases are set equal to 0 at  $z = 0$  is given by:

$$|\psi^{(2)}(0, t)\rangle = \frac{-i}{\hbar} \int_{-\infty}^t dt' \hat{H}_{\text{int}}(t') |\text{vac}\rangle, \quad (\text{A3})$$

where  $|\text{vac}\rangle$  denotes a multimode vacuum state.

For times  $t$  sufficiently long so that the nonlinear interaction is complete, the entangled two-photon state  $|\psi^{(2)}(0, t)\rangle$  can be obtained in the form:

$$\begin{aligned} |\psi^{(2)}(0, t)\rangle = C_\psi \int_{-L}^0 dz \sum_{k_p} \sum_{k_1} \sum_{k_2} \mathcal{E}_p^{(+)}(0, \omega_{k_p} - \omega_p^0) \hat{a}_1^\dagger(k_1) \hat{a}_2^\dagger(k_2) \exp [i(k_p - k_1 - k_2)z] \\ \times \delta(\omega_{k_p} - \omega_{k_1} - \omega_{k_2}) \exp [i(\omega_{k_1} + \omega_{k_2})t] |\text{vac}\rangle. \end{aligned} \quad (\text{A4})$$

The susceptibility  $\chi^{(2)}$  is included in the constant  $C_\psi$ . We note that for times during which the down-converted fields are being created in the crystal, the appropriate wave function differs from that in Eq. (A4). However, detectors are placed at a sufficiently large distance from the output plane of the crystal to assure that such ‘‘partially evolved’’ states cannot be detected.

## APPENDIX B: INTERFERENCE PATTERN FOR AN ARBITRARY PUMP-PULSE PROFILE

We assume an arbitrary complex spectrum  $\mathcal{E}_p^{(+)}(-L, \Omega_p)$  for the envelope of the pump pulse at the input plane of the crystal. We further take into account the effect of second-order dispersion only in the pump beam and assume frequency filters of the same width ( $\sigma_1 = \sigma_2$ ). Under these conditions, the normalized coincidence-count rate  $R_n$  in Eq. (6) can be expressed in terms of the autocorrelation function of the pump field.

Let us introduce the field  $\mathcal{E}_{p\sigma}^{(+)}(z, t)$  according to the definition:

$$\mathcal{E}_{p\sigma}^{(+)}(z, t) = \int_{-\infty}^{\infty} d\Omega_p \mathcal{E}_p^{(+)}(-L, \Omega_p) \exp\left[i\frac{D_p(z+L)}{4\pi}\Omega_p^2\right] \exp\left[-\frac{\Omega_p^2}{\sigma^2}\right] \exp(-i\Omega_p t), \quad (\text{B1})$$

where  $\sigma = \sqrt{2}\sigma_1$ . The above expression describes the propagation of the pump beam through a dispersive material (a multiplicative term describing first-order dispersion is not explicitly included here). Equation (B1) also includes frequency filtering having its origin in the filtering of the down-converted beams and their entanglement with the pump beam.

The two-photon amplitude  $\mathcal{A}_{12, \tau_1}(\tau_1, \tau_2)$  can then be derived from the expression in Eq. (16):

$$\begin{aligned} \mathcal{A}_{12, \tau_1}(\tau_1, \tau_2) &= \frac{C_A}{2} \exp(-i\omega_1^0 \tau_1) \exp(-i\omega_2^0 \tau_2) \\ &\times \sqrt{\pi}\sigma \int_{-L}^0 dz \mathcal{E}_{p\sigma}^{(+)}(z, (\tau_1 + \tau_1 + \tau_2)/2 - \Lambda z) \exp\left[-\frac{\sigma^2}{16}(\tau_1 + \tau_1 - \tau_2 + Dz)^2\right], \end{aligned} \quad (\text{B2})$$

where the parameters  $D$  and  $\Lambda$  are defined in Eq. (32) and the relative time delay  $\tau_l$  of the down-converted beams is introduced in Eq. (34).

The quantity  $\rho$  given in Eq. (7) then has the form (again it is assumed that  $\omega_1^0 = \omega_2^0$ ):

$$\begin{aligned} \rho(\Delta\tau_l) &= \frac{|C_A|^2 \sqrt{2\pi}\pi\sigma}{4R_0} \\ &\times \text{Re} \left\{ \int_{-L/2}^{L/2} dz_1 \int_{-L/2}^{L/2} dz_2 \gamma_\sigma(z_1, z_2, \Lambda(z_1 - z_2)) \exp\left[-\frac{\sigma^2}{8}\left(\Delta\tau_l + \frac{D}{2}(z_1 + z_2)\right)^2\right] \right\}, \end{aligned} \quad (\text{B3})$$

where  $\Delta\tau_l$  is defined in Eq. (33). The correlation function  $\gamma_\sigma(z_1, z_2, x)$  of two pulsed fields at positions  $z_1$  and  $z_2$  is written as

$$\gamma_\sigma(z_1, z_2, x) = \int_{-\infty}^{\infty} dt \mathcal{E}_{p\sigma}^{(+)}(z_1 - L/2, t) \mathcal{E}_{p\sigma}^{(-)}(z_2 - L/2, t + x). \quad (\text{B4})$$

The constant  $R_0$  occurring in Eq. (B3) is expressed as follows:

$$R_0 = \frac{|C_A|^2 \sqrt{2\pi}\pi\sigma}{4} \int_{-L/2}^{L/2} dz_1 \int_{-L/2}^{L/2} dz_2 \gamma_\sigma(z_1, z_2, \Lambda(z_1 - z_2)) \exp\left[-\frac{\sigma^2 D^2}{32}(z_1 - z_2)^2\right]. \quad (\text{B5})$$

For a Gaussian pulse with the complex spectrum as given in Eq. (19), the correlation function  $\gamma_\sigma$  becomes

$$\begin{aligned} \gamma_\sigma(z_1, z_2, \Lambda(z_1 - z_2)) &= \frac{\sqrt{\pi}\tau_{Di}^2}{2\sqrt{1+a_i^2}} \frac{|\xi_p|^2}{\sqrt{\psi(z_1, z_2)}} \exp\left[-\frac{\Lambda^2(z_1 - z_2)^2}{4\psi(z_1, z_2)}\right], \\ \psi(z_1, z_2) &= 2b_i + \frac{2}{\sigma^2} - i\frac{D_p}{4\pi}(z_1 - z_2), \end{aligned} \quad (\text{B6})$$

which, together with Eqs. (B3) and (B5), leads to expressions which agree with those derived from Eqs. (25) and (27). The parameter  $b_i$  is defined in Eq. (30).

The experimental setup without frequency filters ( $\sigma \rightarrow \infty$ ) is of particular interest. In this case, using the identity  $\sqrt{\pi}\sigma \exp(-\sigma^2 y^2/4) \rightarrow 2\pi\delta(y)$  for  $\sigma \rightarrow \infty$ , Eqs. (B3) and (B5) provide a useful expression for the function  $\rho(\Delta\tau_l)$ :

$$\rho(\Delta\tau_l) = \frac{1}{\gamma_\infty(0,0,0)L} \operatorname{Re} \left\{ \int_{-L/2}^{L/2} dz \operatorname{rect}(z/L + 1/2 + 2\Delta\tau_l/(DL)) \right. \\ \left. \times \gamma_\infty(z, -z - 2\Delta\tau_l/D, 2z + 2\Delta\tau_l/D) \right\}, \quad (\text{B7})$$

where  $\operatorname{rect}(x)$  is the rectangular function ( $\operatorname{rect}(x) = 1$  for  $0 < x < 1$  and  $\operatorname{rect}(x) = 0$  otherwise).

- [1] L. Mandel and E. Wolf, *Optical Coherence and Quantum Optics* (Cambridge Univ. Press, Cambridge, 1995).
- [2] J. Peřina, Z. Hradil, and B. Jurčo, *Quantum Optics and Fundamentals of Physics* (Kluwer, Dordrecht, 1994).
- [3] D. N. Klyshko, *Photons and Nonlinear Optics* (Gordon and Breach Science Publishers, New York, 1988).
- [4] A. Joobeur, B. E. A. Saleh, T. S. Larchuk, and M. C. Teich, Phys. Rev. A **53**, 4360 (1996); B. E. A. Saleh, A. Joobeur, and M. C. Teich, Phys. Rev. A **57**, 3991 (1998).
- [5] Z. Y. Ou and L. Mandel, Phys. Rev. Lett. **61**, 50 (1988); Y. H. Shih and C. O. Alley, Phys. Rev. Lett. **61**, 2921 (1988); Z. Y. Ou and L. Mandel, Phys. Rev. Lett. **61**, 54 (1988); J. Brendel, E. Mohler, and W. Martienssen, Phys. Rev. Lett. **66**, 1142 (1991); T. S. Larchuk, R. A. Campos, J. G. Rarity, P. R. Tapster, E. Jakeman, B. E. A. Saleh, and M. C. Teich, Phys. Rev. Lett. **70**, 1603 (1993); A. M. Steinberg, P. G. Kwiat, and R. Y. Chiao, Phys. Rev. Lett. **71**, 708 (1993); C. K. Hong, Z. Y. Ou, and L. Mandel, Phys. Rev. Lett. **59**, 1903 (1987); J. G. Rarity and P. R. Tapster, J. Opt. Soc. Am. B **6**, 1221 (1989); R. Ghosh, C. K. Hong, Z. Y. Ou, and L. Mandel, Phys. Rev. A **34**, 3962 (1986); P. G. Kwiat, K. Mattle, H. Weinfurter, A. Zeilinger, A. V. Sergienko, and Y. Shih, Phys. Rev. Lett. **75**, 4337 (1995); P. W. Milloni, H. Fearn, and A. Zeilinger, Phys. Rev. A **53**, 4556 (1996).
- [6] M. D. Reid and D. F. Walls, Phys. Rev. A **34**, 1260 (1986); P. R. Tapster, J. G. Rarity, and P. C. M. Owens, Phys. Rev. Lett. **73**, 1923 (1994); T. B. Pittman, Y. H. Shih, A. V. Sergienko, and M. H. Rubin, Phys. Rev. A **51**, 3495 (1995); P. R. Tapster, J. G. Rarity, and P. C. M. Owens, Phys. Rev. Lett. **73**, 1923 (1994).
- [7] T. B. Pittman, Y. H. Shih, D. V. Strekalov, and A. V. Sergienko, Phys. Rev. A **52**, R3429 (1995); T. B. Pittman, D. V. Strekalov, D. N. Klyshko, M. H. Rubin, A. V. Sergienko, and Y. H. Shih, Phys. Rev. A **53**, 2804 (1996); D. V. Strekalov, A. V. Sergienko, D. N. Klyshko, and Y. H. Shih, Phys. Rev. Lett. **74**, 3600 (1995); B. M. Jost, A. V. Sergienko, A. F. Abouraddy, B. E. A. Saleh, and M. C. Teich, Opt. Express **3**, 81 (1998); M. C. Teich and B. E. A. Saleh, Čs. čas. fyz. **47**, 3 (1997), in Czech.
- [8] J. D. Franson, Phys. Rev. A **44**, 4552 (1991); J. G. Rarity and P. R. Tapster, Phys. Rev. A **45**, 2052 (1992); A. V. Sergienko, M. Atature, B. M. Jost, J. Peřina, Jr., B. E. A. Saleh, and M. C. Teich, Quantum Cryptography with Femtosecond Parametric Down Conversion, 1998 OSA Ann. Meeting Program (Baltimore, MD), Oct. 4-9, 1998, p. 104.
- [9] D. M. Greenberger, M. A. Horne, A. Shimony, and A. Zeilinger, Am. J. Phys. **58**, 1131 (1990).
- [10] D. M. Greenberger, M. A. Horne, and A. Zeilinger, Phys. Today **46** (8), 22 (1993); S. P. Tewari and P. Hariharan, J. Mod. Opt. **44** 543 (1997); D. A. Rice, C. F. Osborne, and P. Lloyd, Phys. Lett. A **186**, 21 (1994); M. D. Reid and W. J. Munro, Phys. Rev. Lett. **69**, 997 (1992); D. N. Klyshko, Phys. Lett. A **172**, 399 (1993); J. A. Bergou and M. Hillery, Phys. Rev. A **55**, 4585 (1997); C. C. Gerry, Phys. Rev. A **53**, 4591 (1996).
- [11] M. Zukowski, A. Zeilinger, M. A. Horne, and A. K. Ekert, Phys. Rev. Lett. **71**, 4287 (1993); A. Zeilinger, M. A. Horne, H. Weinfurter, and M. Zukowski, Phys. Rev. Lett. **78**, 3031 (1997); J.-W. Pan and A. Zeilinger, Phys. Rev. A **57**, 2208 (1998).
- [12] D. Bouwmeester, J.-W. Pan, K. Mattle, M. Eibl, H. Weinfurter, and A. Zeilinger, Nature **390**, 575 (1997).
- [13] G. Di Giuseppe, L. Haiberger, F. De Martini, and A. V. Sergienko, Phys. Rev. A **56**, R21 (1997).
- [14] T. E. Keller and M. H. Rubin, Phys. Rev. A **56**, 1534 (1997).
- [15] W. P. Grice and I. A. Walmsley, Phys. Rev. A **56**, 1627 (1997); W. P. Grice, R. Erdmann, I. A. Walmsley, and D. Branning, Phys. Rev. A **57**, R2289 (1998).
- [16] Z. Y. Ou, Quant. and Semiclass. Optics **9**, 599 (1997).
- [17] C. K. Hong, Z. Y. Ou, and L. Mandel, Phys. Rev. Lett. **59**, 2044 (1987).
- [18] T. S. Larchuk, M. C. Teich, and B. E. A. Saleh, Phys. Rev. A **52**, 4145 (1995).
- [19] B. E. A. Saleh and M. C. Teich, *Fundamentals of Photonics* (Wiley, New York, 1991).
- [20] J.-C. Diels and W. Rudolph, *Ultrashort Laser Pulse Phenomena* (Academic Press, San Diego, 1996).